ACS OMEGA

Open Access

http://pubs.acs.org/journal/acsodf

Article

Danhong Injection Inhibits Apoptosis in Ischemia/Reperfusion Injury Based on Network Pharmacology Analysis, Molecular Docking, and Experimental Verification

Shennan Shi, Yalan Lu, Qiwen Long, Yanqing Wu, Yan Guo, Nipi Chen, Haitong Wan, and Bo Jin*

Cite This: *ACS Omega* 2025, 10, 9604−9612

Read Online

ACCESS | Metrics & More | Article Recommendations | Supporting Information

ABSTRACT: Danhong injection (DHI), a Chinese patent compound injection, is widely used in the treatment of cardiovascular diseases (CVD) in China. However, the underlying mechanisms have not been fully elucidated. This study investigated the therapeutic effect and the underlying mechanisms of DHI against ischemia-reperfusion (I/R) injury and endothelial dysfunction (ED). Network pharmacology analysis revealed that DHI had six core active compounds (Danshensu, salvianolic acid A, salvianolic acid B, rosmarinic acid, protocatechualdehyde, and caffeic acid) and 19 potential targets in treating I/R injury. Notably, the regulation of apoptosis was significantly enriched, as indicated by the results of the gene ontology (GO) enrichment analysis. Molecular docking studies confirmed that these targets had high affinity with the active compounds of DHI. Finally, experimental validation in vivo and in vitro demonstrated that DHI could mitigate I/R injury and ED, potentially by reducing oxidative damage through the inhibition of apoptosis via the PTEN/AKT pathway. These findings significantly advance our understanding of the molecular mechanisms in DHI treatment and contribute further to promoting the clinical application of CVD.

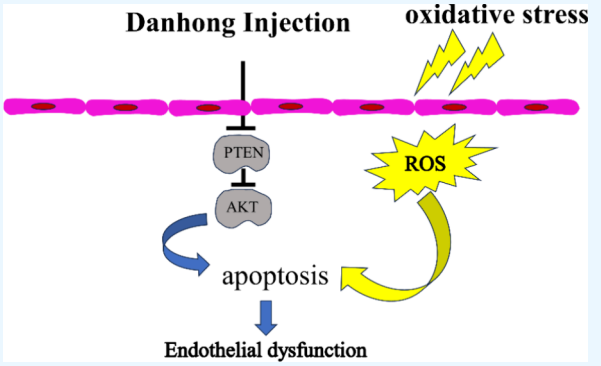

1. INTRODUCTION

Ischemic heart disease and ischemic stroke are the leading causes of death in cardiovascular diseases (CVD), and timely blood supply therapy is a classic strategy. Unfortunately, tissues may undergo temporary ischemia, followed by a sudden restoration of blood supply, which can damage the mitochondrial electron transport chain and disrupt oxidative phosphorylation. This disruption leads to an increase in the generation of reactive oxygen species (ROS), ultimately triggering cell death. This pathophysiological process is known as ischemia/reperfusion (I/R) injury.[1,2] Vascular endothelial cells are located in the first layer inner surface of vessels, so they will be the first to be attacked by I/R injury.[3] Studies have shown that oxidative stress-induced endothelial dysfunction (ED) is recognized as a contributing factor in the development of I/R injury.[4] The imbalance between oxidants and antioxidants in cells can disrupt redox signaling and cause molecular damage, leading to a range of phenotypic changes, including altered gene expression, arrested cell proliferation and growth, cellular senescence, and cell death, ultimately resulting in ED.[5,6] Hence, protecting endothelial cells against oxidative stress may be an essential element in treating the development or progression of ischemic CVD.[7]

Danhong injection (DHI), a traditional Chinese medicine, is a compound derived from Radix *Salvia miltiorrhiza* Bge. (Labiatae, Danshen in Chinese) and *Carthamus tinctorius* L. (Compositae, Honghua in Chinese),[8] which has been widely employed in the treatment of CVD for many years.[9,10] Previous studies have demonstrated that DHI exhibits various pharmacological effects, including anti-inflammatory, hypolipidemic, anticoagulant, antithrombotic, and antioxidant properties.[11−14] Our previous studies have found that DHI and its active ingredients can inhibit autophagy induced by oxidative stress.[15] Therefore, the present study employed network pharmacology combined with molecular docking verification and experimental validation to clarify the possible mechanisms of DHI against I/R injury and ED, providing data to support further investigation into the mechanisms of the primary active components of DHI in ameliorating I/R injury.

2. RESULTS

2.1. Identification of Chemical Constituents in DHI.

Based on the screening criteria, 87 active compounds of DHI were collected from the TCMSP database and literature, as

Received: November 30, 2024
Revised: February 15, 2025
Accepted: February 19, 2025
Published: February 25, 2025

https://doi.org/10.1021/acsomega.4c10868
ACS Omega 2025, 10, 9604−9612

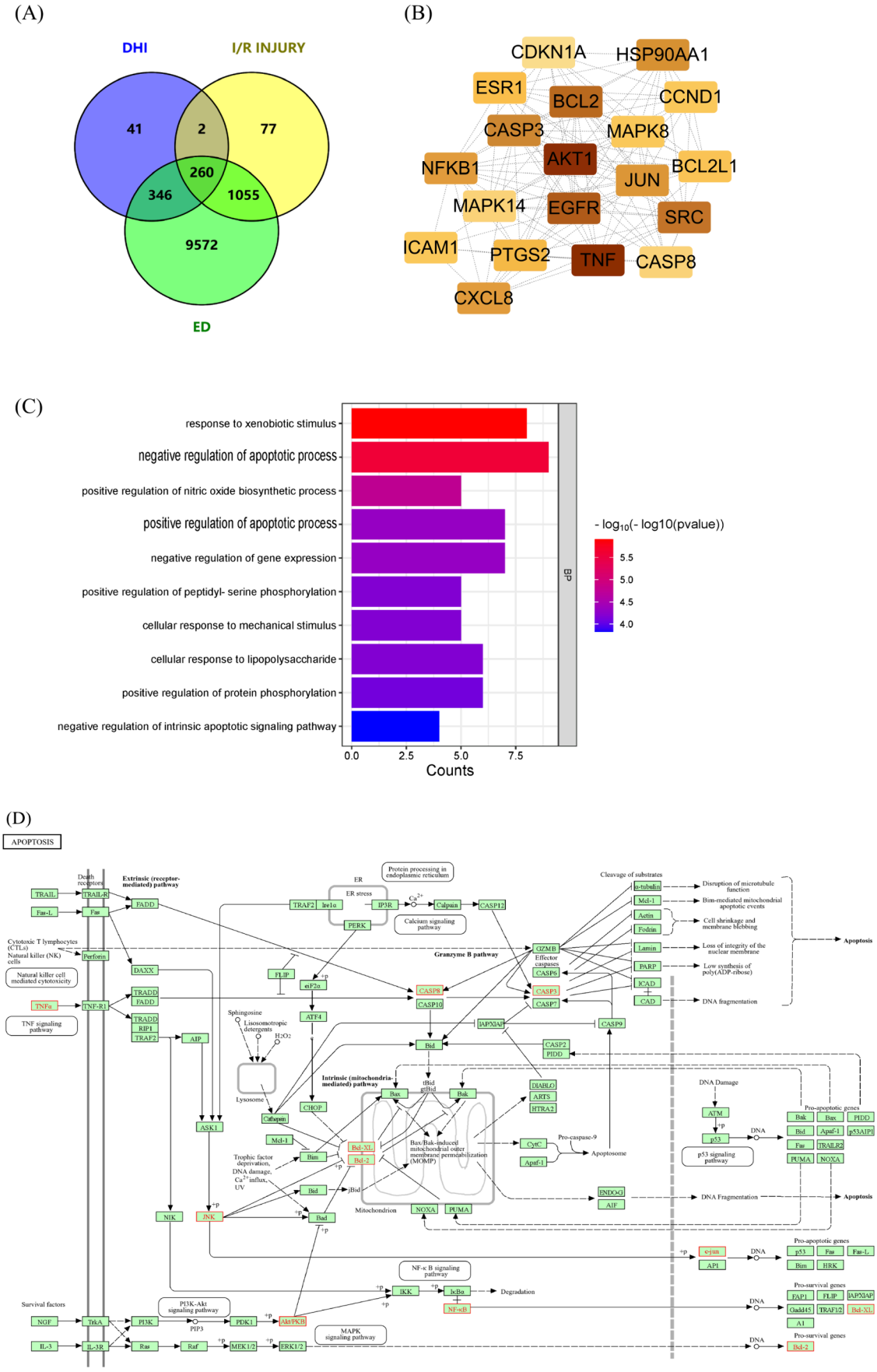

Figure 1. Results of PPI network analysis of DHI interfering with I/R injury and ED intersection targets. (A) Common targets of DHI, I/R injury, and ED. (B) Process of identifying 19 hub genes. (C) GO terms in the BP category. (D) KEGG analysis of apoptosis.

https://doi.org/10.1021/acsomega.4c10868
ACS Omega 2025, 10, 9604−9612

shown in Supporting Information Table S1. The chromatographic fingerprint of DHI was established using high-performance liquid chromatography (HPLC).[16] According to a previous experiment, we chose six primary active substances in qualified DHI, including Salvianic acid A (danshensu, C9H9O5), Protocatechuicaldehyde (C7H6O3), Rosmarinic acid (C18H16O8), Caffeic acid (C9H8O4), Salvianolic acid B (C36H30O16) and Salvianolic acid A (C26H22O10).

2.2. Network Pharmacology Analysis. *2.2.1. Protein−Protein Interaction Network and Hub Genes.* According to three databases—DisGeNET, GeneCards, and OMIM—the number of confirmed or potential targets for I/R injury and ED. All targets were screened and standardized using the STRING database, resulting in 1507 and 11,270 remaining targets after removing duplicates. Ultimately, 260 common targets were identified as candidate targets for improving I/R injury and ED through DHI (Figure 1A).

To identify the key components and core targets of DHI for improving I/R injury and ED, PPI interconnection network information on 260 overlapping targets was obtained through the STRING database after excluding unconnected targets (Supplementary Figure S2). The network was then visualized by using Cytoscape. Furthermore, we employed the MOCDE plugin in Cytoscape to identify the hub targets. Then, 19 hub targets were identified using the Cytoscape. The significance of these indicators is represented by the color of the nodes, with darker nodes indicating greater importance (Figure 1B)

2.2.2. Enrichment Analysis. Gene Ontology (GO) enrichment analyses were conducted using the 19 targets shared by DHI, ED, and I/R injury. The biological processes (BP) associated with DHI intervention in I/R injury and ED included response to xenobiotic stimulus, negative regulation of the apoptotic process, positive regulation of nitric oxide biosynthetic process, negative regulation of gene expression, and positive regulation of apoptotic process (Figure 1C). The cellular components (CC) predominantly involved the protein-containing complex, mitochondrion, cytoplasm, nucleoplasm, and cytosol (Supplementary Figure S3). The molecular functions (MF) encompassed enzyme binding, ubiquitin protein ligase binding, nitric-oxide synthase regulator activity, identical protein binding, and protein phosphatase binding (Supplementary Figure S4).

By combining the results of enrichment analysis, we concentrated on the effects of apoptosis on I/R injury and ED, investigating how DHI can mitigate these conditions by influencing the apoptotic processes. We explored the regulation of the apoptosis pathway (hsa04210). The apoptosis pathway was drawn by KEGG (https://www.genome.jp/) (Figure 1D).

2.2.3. Molecular Docking Validation. The AutoDockTools software was utilized for molecular docking to validate the reliability of the findings obtained through network pharmacology. Affinity < −5.0 kcal·mol^{-1} implies good binding activity; affinity < −7.0 kcal·mol^{-1} suggests strong docking activity. Using PyMOL, the six core bioactive compounds were observed to enter the active pockets of three receptors, respectively. Docking parameters and details of compounds and targets are presented in Table 1. Combined with KEGG analysis and GO enrichment analysis, we have focused on two targets: AKT1 and BCL-2. The two- and three-dimensional conformations of these representative complexes, along with representative examples, are illustrated in Figure 2A,B.

Table 1. Affinity (kcal/mol) of Molecular Docking Simulation

bioactive compounds	AKT1	BCL-2
caffeic acid	−5.3	−5.9
danshensu	−5.3	−5.8
protocatechualdehyde	−4.7	−5.2
rosmarinic acid	−6.2	−6.4
salvianolic acid A	−6.3	−6.7
salvianolic acid B	−6.3	−7.7

2.3. DHI Improved Antioxidant Activity in MCAO Rats. MCAO rats were established; the infarct size decreased following DHI administration (Supplementary Figure S5), and serum was collected to investigate the impact of DHI on antioxidant activity in I/R injury. The MDA level significantly increased following I/R injury ($P < 0.01$). However, after DHI treatment (1 mL/kg), the MDA levels were significantly reversed ($P < 0.01$) (Figure 3A). The production of SOD and GSH/GSSG ($P < 0.05$) in the MCAO group decreased, which was compared to the sham group. Following treatment with DHI, the levels of SOD and the GSH/GSSG ratio ($P < 0.05$) increased in comparison to the MCAO group (Figure 3B, C).

2.4. DHI Regulated Apoptosis-Related Protein Expression in MCAO Rats. The expression of the apoptosis-related proteins BCL-2 and BAX were determined using Western blot analysis. Compared to the control group, the expression of BAX protein in MCAO rats was significantly increased ($P < 0.01$), while the expression of BCL-2 protein was significantly decreased ($P < 0.01$). Following DHI treatment, the expression levels of BAX and BCL-2 were reversed (Figure 3D−G).

According to the key genes of the hsa04210 pathway, we assessed the expression levels of the AKT and PTEN proteins. As shown in Figure 3H−J, the expression of AKT (phospho T308) protein in the MCAO group was significantly lower than that in the sham group ($P < 0.01$), while the expression of PTEN protein was elevated. Following DHI treatment, the expression of AKT (phospho T308) protein significantly increased ($P < 0.05$), and the expression of the PTEN protein decreased ($P < 0.01$).

2.5. DHI Treatment Inhibited the Cell Viability and Increased Cell Proliferation Rate in H_2O_2-Induced HUVECs. The cytotoxicity of H_2O_2 on HUVECs was evaluated, and we detected that the cell viability gradually decreased after exposure to H_2O_2, and a significant decrease was found at 200 μM ($P < 0.05$) (Figure 4A). Therefore, 200 μM H_2O_2 was selected as the optimum concentration for the following experiments. The results of the MTT assay indicated that the concentrations 0.5−5 μL/mL DHI did not affect the cell viability on HUVECs (Figure 4B) and 0.1−1 μL/mL DHI significantly increased the loss of cell viability induced by H_2O_2 ($P < 0.05$) (Figure 4C). Therefore, DHI concentrations of 0.5 and 1 μL/mL were selected for all subsequent experiments.

The EdU detection results indicated that the cell proliferation rate significantly decreased following H_2O_2 treatment ($P < 0.01$). In contrast, DHI treatment was able to reverse the decrease in the cell proliferation rate caused by H_2O_2 ($P < 0.05$) (Figure 4D).

2.6. DHI Improved Antioxidant Activity in H_2O_2-Induced HUVECs. We also examined the MDA content, SOD activity, and GSH/GSSG ratio within cells. As shown in Figure 4E, the levels of MDA were significantly increased in the

https://doi.org/10.1021/acsomega.4c10868
ACS Omega 2025, 10, 9604−9612

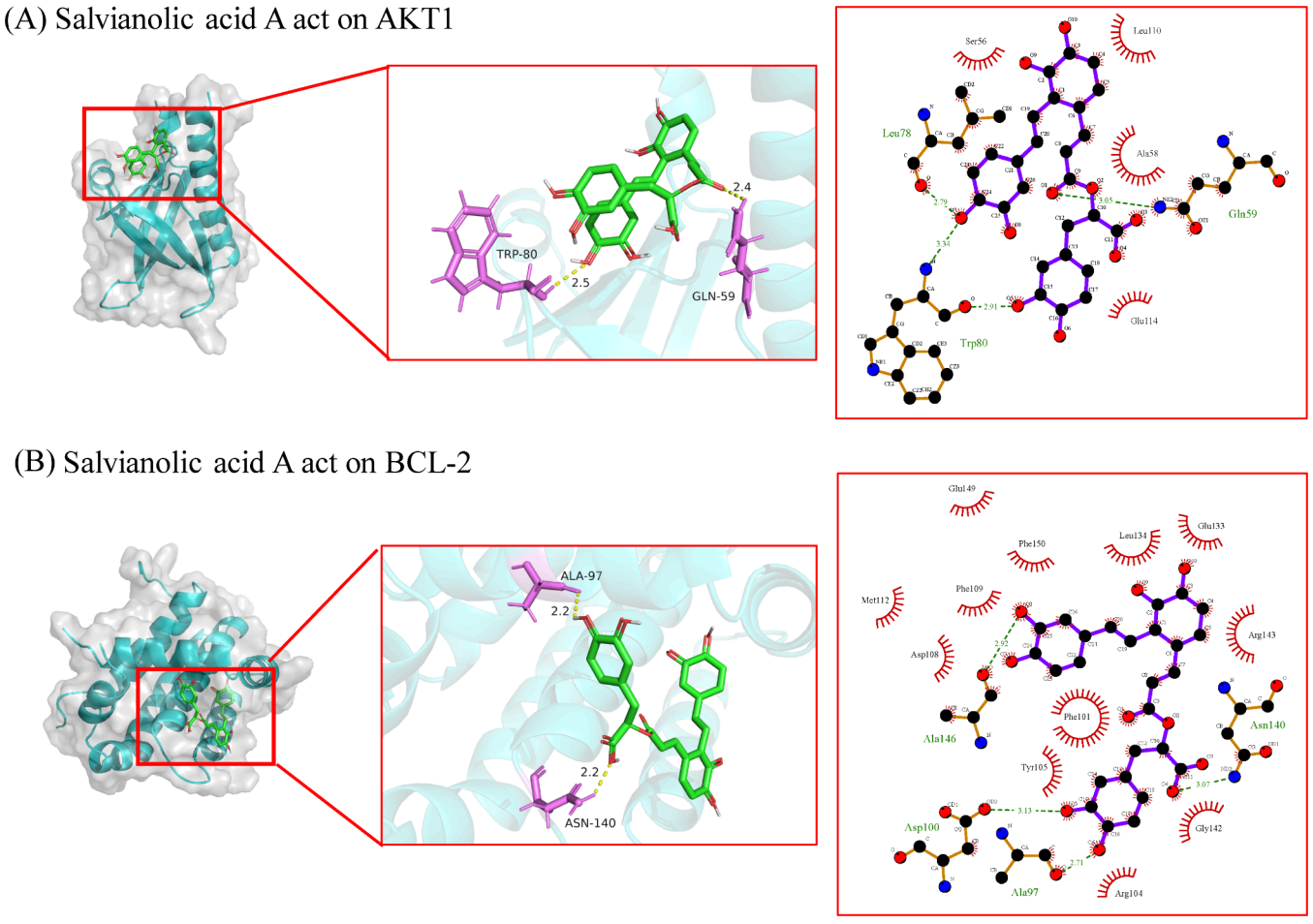

Figure 2. Heat map of molecular docking results. (A) Salvianolic acid A acts on AKT1. (B) Salvianolic acid A act on BCL-2.

H_2O_2-treated group ($P < 0.05$), which could be reversed by DHI treatment ($P < 0.05$). Additionally, H_2O_2 treatment led to a significant decrease in the activity of SOD and the ratio of GSH/GSSG compared to the control group ($P < 0.01$), and DHI treatment significantly enhanced the SOD activity and GSH/GSSG compared with the H_2O_2-treated group ($P < 0.05$) (Figure 4F, G).

As displayed in Figure 4H, the level of ROS in the H_2O_2-treated group was significantly elevated compared to that in the control group ($P < 0.01$), and it was inhibited in the DHI treatment group (0.5 μL/mL) ($P < 0.01$).

2.7. DHI Inhibited Apoptosis in H_2O_2-Induced HUVECs. The flow cytometry results indicate that the apoptosis rate significantly increased following H_2O_2 treatment compared to the control group, but was lower in cells treated with DHI (Figure 5A). Compared with the control group, the expression level of BAX in the H_2O_2 group was significantly increased ($P < 0.05$), while the expression level of BCL-2 was significantly decreased ($P < 0.05$). In contrast to the H_2O_2 group, the expression of BAX significantly decreased, and the expression of BCL-2 and BCL-2/BAX significantly increased in the 0.5 μL/mL DHI group (Figure 5B–E). Western blot analysis also demonstrated that the expression of AKT (phospho T308) protein in the H_2O_2 group was significantly lower than that in the control group ($P < 0.05$), while the expression of PTEN protein was significantly increased ($P < 0.05$) Figures 5F–H). Following DHI treatment, these effects were reversed ($P < 0.05$).

3. DISCUSSION

I/R injury is an unavoidable complication in the treatment of ischemic stroke.[17] Identifying a safe and effective treatment method is crucial for reducing the mortality associated with this condition. DHI is one of the most commonly used injectable medications for treating ischemic stroke.[18] Studies have reported that oxidative stress-induced ED plays a significant role in the onset and progression of I/R injury.[19] Our previous research demonstrated that DHI can protect endothelial cells from oxidative stress; however, the specific protective mechanisms remain unclear. Therefore, this experiment was conducted to investigate the protective effect of DHI on I/R injury and ED and its potential molecular mechanisms. This was achieved by integrating network pharmacology, molecular docking, and experimental validation.

According to the results of the GO enrichment analysis, 19 hub genes are significantly associated with the regulation of apoptosis. Molecular docking studies indicated that the active compounds in DHI exhibited a strong binding affinity to the corresponding targets associated with the apoptosis pathway. This suggests that the therapeutic effects of DHI on I/R injury and ED may be associated with the apoptosis pathway. Furthermore, the apoptosis pathway was visualized using a bioinformatics platform, revealing that AKT1 and BCL-2 are key targets related to apoptosis.

DHI, due to its unique injection characteristics, exerts some of its therapeutic effects through endothelial cells. Therefore, a rat model of MCAO and H_2O_2-induced HUVECs model was

https://doi.org/10.1021/acsomega.4c10868
ACS Omega 2025, 10, 9604−9612

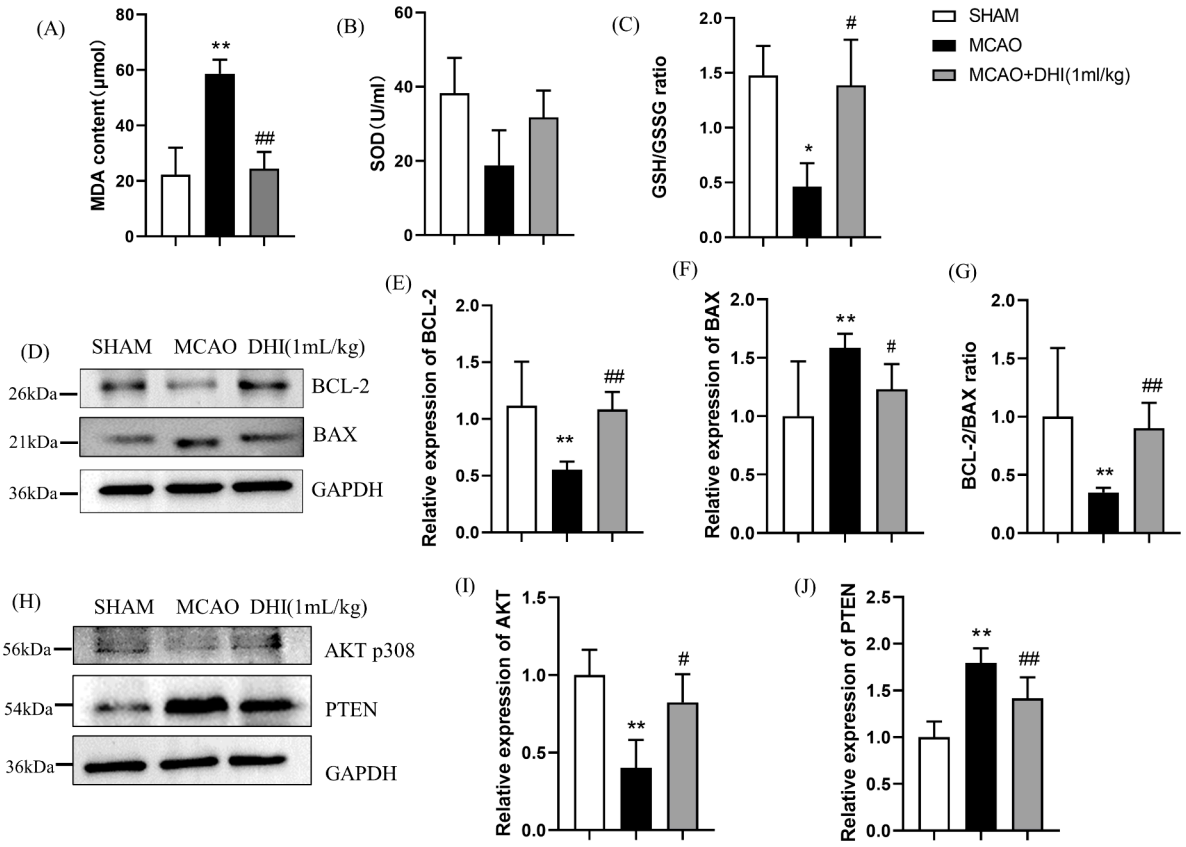

Figure 3. Effect of DHI on oxidative stress and apoptosis in MACO rats. (A) Effect of DHI on the MDA level. (B) Effect of DHI on the SOD level. (C) Effect of DHI on the GSH/GSSG level. (D) Respective blots of BAX and BCL-2. (E) Effect of DHI on the BCL-2 expression. (F) Effect of DHI on the BAX expression. (G) Effect of DHI on the BCL-2/BAX ratio. (H) Respective blots of AKT (phospho T308) and PTEN. (I) Effect of DHI on AKT (phospho T308) expression. (J) Effect of DHI on PTEN expression. Values are presented as mean ± SD (n = 3). $^{*}P < 0.05$, $^{**}P < 0.01$ vs SHAM group. $^{\#}P < 0.05$, $^{\#\#}P < 0.01$ vs MCAO group.

utilized to evaluate the potential impact of DHI on I/R injury and ED. The experiments in vivo and in vitro demonstrated that DHI effectively alleviated brain I/R injury and HUVECs cell viability. Additionally, DHI improved antioxidative stress in the MCAO rats and H_2O_2-induced HUVECs. These findings suggest that DHI may provide protective effects by inhibiting lipid peroxidation and restoring antioxidant levels.

AKT1 is an isoform of AKT, and both are closely associated with apoptosis.[20] PTEN is an important tumor suppressor gene primarily involved in regulating signal transduction pathways related to cell survival and cell death.[21] It is considered an inhibitor of the AKT signaling pathway and suppresses the expression of AKT.[22] Once AKT is activated, it can effectively inhibit apoptosis and promote cell growth by further regulating the expression of downstream transcription factors or antiapoptotic factors, such as those in the BCL family.[23] BCL-2 and BAX are the two main members of the BCL-2 gene family. BCL-2 inhibits apoptosis, while BAX plays a pro-apoptotic role.[24] As marker proteins of apoptosis, they play a crucial role in the signaling regulation of the apoptosis pathway.[25,26] DHI treatment significantly increased the levels of BCL-2 in rat cardiac tissue while suppressing the expression of BAX and caspase-3, thereby exerting a cardioprotective effect.[27] In our study, we obtained similar findings, indicating that DHI not only exerts cardioprotective effects by inhibiting cell apoptosis but also plays a role in protecting against I/R injury and ED through the inhibition of cell apoptosis.

Based on the experimental results and network analysis, DHI may alleviate I/R injury and ED by regulating oxidative stress-induced apoptosis. However, further studies are needed to elucidate the antiapoptotic mechanisms of DHI and the regulation of the PTEN/AKT pathway.

4. CONCLUSIONS

Network pharmacology analysis suggests that DHI plays a significant role in I/R injury and ED through various compounds, targets, and pathways. Molecular docking studies, along with experimental verification, confirm that DHI exerts its protective effects primarily by modulating the apoptosis pathway. The findings of this study provide a theoretical foundation for the application of DHI in the treatment of an ischemic stroke.

5. MATERIALS AND METHODS

5.1. Tools, Databases, and Reagents. STRING: https://string-db.org/; Traditional Chinese Medicine System Pharmacology (TCMSP): https://old.tcmsp-e.com/tcmsp.php; SwissTargetPrediction: http://swisstargetprediction.ch/; PubChem: https://pubchem.ncbi.nlm.nih.gov/; Protein Data Bank (RCSB PDB): https://www.rcsb.org/; Database for Annotation, Visualization, and Integrated Discovery (DAVID): https://david.ncifcrf.gov; OMIM database: https://omim.org/; DisGeNET database: https://www.disgenet.org/; GeneCards database: http://www.genecards.org/; Venn diagram: http://www.bioinformatics.com.cn/; BATMAN-TCM: http://bionet.

https://doi.org/10.1021/acsomega.4c10868
ACS Omega 2025, 10, 9604−9612

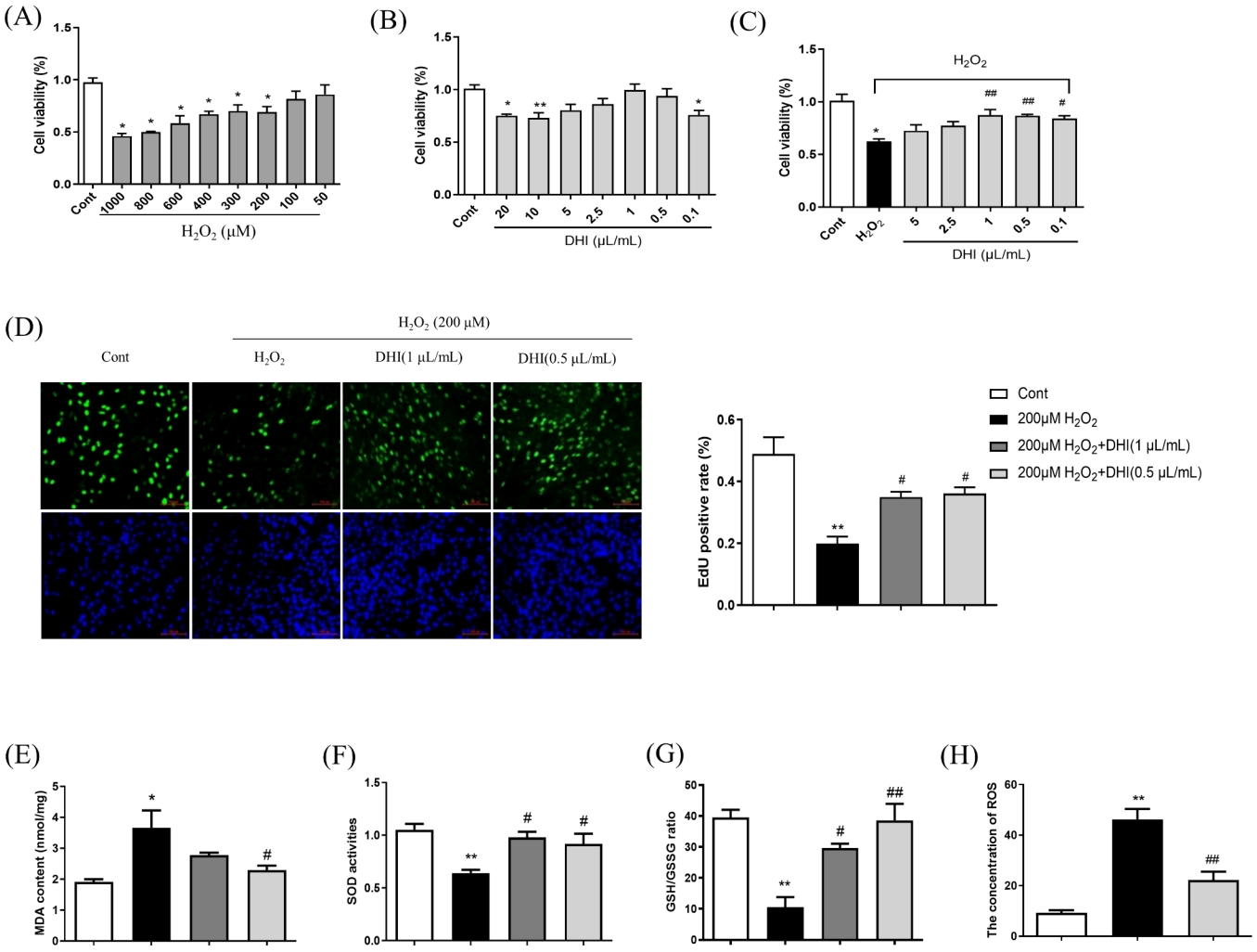

Figure 4. Effects of DHI on cell viability, proliferation rate and oxidative stress in H_2O_2-induced HUVECs. (A) HUVECs were exposed to different concentration of H_2O_2 for 2 h. (B) HUVECs were treated with different concentration of DHI for 24 h. (C) HUVECs were processed with various concentrations of DHI for 24 h after treated with H_2O_2. (D) Percentage of EdU-positive cells of H_2O_2-induced HUVECs after DHI treatment for 24 h by EdU staining (20×). (E) Effect of DHI on the MDA level. (F) Effect of DHI on the SOD level. (G) Effect of DHI on the GSH/GSSG level. (H) Effect of DHI on the ROS level. Values are presented as the mean ± SD $^*P < 0.05$, $^{**}P < 0.01$ vs Control group; $^{\#}P < 0.05$, $^{\#\#}P < 0.01$ vs H_2O_2 group.

ncpsb.org.cn/; Cytoscape v3.10.1; AutoDockTools v1.5.6; PyMOL v2.6.0. DHI was supplied by Heze Buchang Pharmaceutical Co. Roswell Park Memorial Institute (RPMI) 1640 and fetal bovine serum (FBS) was produced by Gibco BRL (CA, United States). The MTT assay kit was purchased from Sigma (St. Louis, United States). FITC-Annexin V apoptosis detection kit (556547) was obtained from BD Biosciences (NJ, United States). RIPA lysis buffer (P0013B), PMSF (ST506), BCA (P0009), EdU (C0071S), ROS (S0033S), Malondialdehyde (MDA, S0131S), Superoxide Dismutase (SOD, S0101S), and GSH/GSSG (S0053) assay kits were purchased from Beyotime Biotechnology (Shanghai, China). Antibodies specific for BAX (UniProtKB Q07812, cat. ab32503, 1:1000, Abcam), BCL-2 (UniProtKB P10415, cat. ab32124, 1:1000, Abcam), AKT (phospho T308) (UniProtKB P31749, cat. ab38449, 1:1000, Abcam), PTEN (UniProtKB P60484, cat. ab32199, 1:1000, Abcam), and GAPDH (UniProtKB P46406, cat. ab8245, 1:2000, Abcam) were obtained from Abcam (Cambridge, United Kingdom). Goat Anti-Rabbit IgG H&L (cat. ab97051) and Goat Anti-Mouse IgG H&L (cat. ab6789) were obtained from Abcam (Cambridge, United Kingdom).

5.2. Identifying Potential Gene Targets of ED Caused by I/R Injury. Potential therapeutic targets of I/R injury and ED were excavated from the OMIM database, DisGeNET database, and GeneCards database, using the keywords "ischemia/reperfusion injury" and "endothelial dysfunction". The disease targets were standardized as Gene Symbols by using the STRING database.

5.3. Screening of Active Compounds and Action Targets of DHI. The active compounds in DHI were screened from the TCMSP database and the published literature. The screening criteria were OB ≥ 30% and DL ≥ 0.18. Additionally, low DL values but values high and concentrations with pharmacological effects were also adopted as considered active components. Canonical SMILES structures were from PubChem while potential targets were obtained in identified using SwissTargetPrediction and BATMAN-TCM. Subsequently, the protein targets were entered into the STRING database for normalization using "*Homo sapiens*".

https://doi.org/10.1021/acsomega.4c10868
ACS Omega 2025, 10, 9604−9612

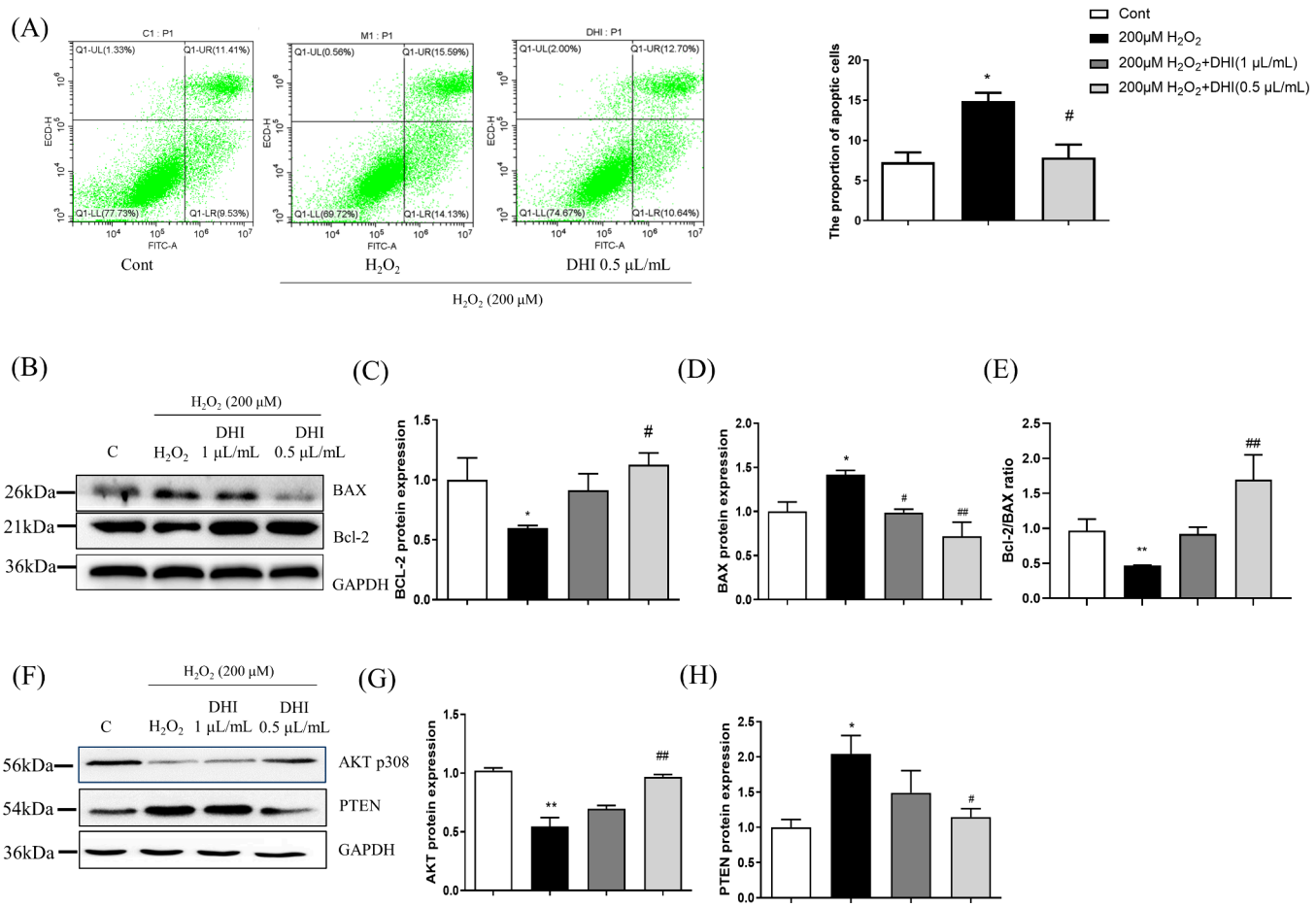

Figure 5. Effect of DHI on apoptosis in H_2O_2-induced HUVECs. (A) Apoptosis cells are shown in the Q1-LR quadrant of each plot. (B) Respective blot of BAX and BCL-2. (C) Effect of DHI on BCL-2 expression. (D) Effect of DHI on BAX expression. (E) Effect of DHI on the BCL-2/BAX ratio. (F) Respective blot of AKT (phospho T308) and PTEN. (G) Effect of DHI on AKT (phospho T308) expression. (H) Effect of DHI on PTEN expression. Values are presented as mean ± SD (n = 3). *P < 0.05, **P < 0.01 vs Control group. $^{\#}P$ < 0.05, $^{\#\#}P$ < 0.01 vs H_2O_2 group.

5.4. Construction of the Protein−Protein Interaction (PPI) and Hub Genes Network. The overlapping proteins between DHI and diseases were uploaded to the STRING database to generate a PPI network analysis, where unconnected targets were eliminated, and other parameters were kept at default settings. The results were visualized using Cytoscape, and the hub genes were identified with the MOCDE tool integrated within Cytoscape. Then, the STRING database was used to construct the PPI network, which was visualized by using Cytoscape.

5.5. Enrichment Pathway Analysis. The hub genes were input into the DAVID database to further explore hub genes and potential functional modules for Gene Ontology (GO) enrichment analysis. The results were visualized by using an online platform for data analysis and visualization (https://www.bioinformatics.com.cn/).

5.6. Molecular Docking Validation. Molecular docking between the core components and the core targets was conducted based on the aforementioned analysis. The three-dimensional crystal structures of the target proteins were retrieved from the RCSB PDB. Docking parameters and the details of the targets are presented in Table 2. The corresponding PDB format files were downloaded, dewatered, and hydrogenated using AutoDockTools. These files were then selected as receptors and saved in PDBQT format. The MOL2 files of the active components were obtained from the TCMSP database, hydrogenated in AutoDockTools, designated as ligands, and exported as PDBQT files. Molecular docking was performed using AutoDock Vina. Components and targets exhibiting strong binding activity were screened based on their affinity and visualized using PyMOL.

Table 2. Docking Parameters of the Corresponding Apoptosis Pathway-Related Targets

		center coordinates (X, Y, Z)			size (X, Y, Z)		
gene	PDB ID	X	Y	Z	X	Y	Z
AKT1	1UNQ	19.8	21.0	4.6	24.8	25.5	43.3
BCL2	4LXD	23.6	33.5	9.0	21.8	28.5	23.1

5.7. Experimental Verification. *5.7.1. Animals and Treatment.* Adult male Sprague−Dawley rats (280−300 g) (No. IACUC-20210412-08) were obtained from the Experimental Animal Center of Zhejiang Chinese Medical University. All rats were maintained in a temperature-controlled room (25 °C ± 1) with a 12 h light cycle fed with distilled water and a standard diet. All animal experiments were performed in accordance with the animal welfare and ethics guidelines of the Institutional Animal Care and Use Committee and approved by the Animal Care and Use Committee of Zhejiang Chinese Medical University (No.

https://doi.org/10.1021/acsomega.4c10868
ACS Omega 2025, 10, 9604−9612

20210412). This study is reported in accordance with Animal Research: Reporting of In Vivo Experiments guidelines.

5.7.2. Middle Cerebral Artery Occlusion (MCAO) Model Establishment. After anesthesia, a 3-0 nylon suture with a silicone-coated tip was inserted into the right common carotid artery and advanced through the internal carotid artery to occlude the middle cerebral artery (MCA). The occlusion was maintained for 2h, and then the suture was removed to allow reperfusion for 24 h. Sham-operated rats were subjected to the same surgical procedure, but the MCA was not occluded. Rats were randomly divided into three groups: sham-operated (SHAM), MCAO, and DHI. The volume of DHI administered was 1 mL/kg. One hour after the onset, the rats received either saline or DHI via vein injection. Blood was centrifuged at 4000 rpm for 10 min, and separated serum was stored in Eppendorf tubes stored at −80 °C.

5.7.3. Cells Culture and Treatment. The HUVECs were purchased from the Institute of Biology, Chinese Academy of Sciences (Shanghai, China). HUVECs were cultured in RPMI 1640 medium supplemented with 10% fetal bovine serum and 1% penicillin-streptomycin at 37 °C in a humidified atmosphere of 5% CO_2, subculture at 80% of the bottom of the culture bottle.

The cells were divided into four groups, Control group (Cont): HUVECs were placed within a 6-well plate (3×10^5 cells/well), Cultured with normal medium; H_2O_2 group: after 24 h, HUVECs were induced by exposure to H_2O_2 for 2 h; DHI group: HUVECs were exposed to H_2O_2 for 2 h before being treated with two concentrations of DHI (1, 0.5 μL/mL) for 24 h.

5.7.4. MTT Assay. Briefly, cells were seeded in a 96-well plate at a density of 1×10^4 cells per well. Following various treatments, 10 μL of MTT was added to each well and incubated at 37 °C for 4 h. Subsequently, the supernatant was discarded, and the formazan crystals were dissolved in 150 μL of DMSO. After being incubated for 10 min, the absorbance was measured at 490 nm using a microplate reader (Bio Tek, USA).

5.7.5. EdU Assay. BeyoClick EdU Cell Proliferation Kit for Imaging, Alexa Fluor 488 dye was used for detecting cells after treatment, according to the manufacture's protocol.

5.7.6. GSH/GSSG Ratio, Activity of SOD, and MDA Levels. The cell homogenate and blood samples were prepared according to the kit instructions. The GSH/GSSG, SOD, and MDA assays were performed by using the commercial kits.

5.7.7. Intracellular ROS Measurement. The HUVECs were collected and washed three times with cold PBS. Subsequently, the cells were incubated with DCFH-DA (10 μM) at 37 °C for 20 min in the dark, followed by two washes with PBS. The relative fluorescence intensity of the cells was measured using flow cytometry.

5.7.8. Western Blot. After treatment, total protein was extracted from the cells and brain tissue using RIPA lysis buffer containing 1 mM PMSF. The protein concentration was determined using a BCA assay kit. Proteins from each sample were separated by SDS-PAGE gel electrophoresis and subsequently transferred to a PVDF membrane. The PVDF membrane was incubated overnight at 4 °C with primary antibodies against BAX, BCL-2, AKT (phospho T308), PTEN, and GAPDH. Following this, the membrane was incubated with a secondary antibody for 2 h. Membranes were scanned by using a chemiluminescent detection system. Each experiment was repeated three times by following the same procedure to obtain an average value.

5.7.9. Flow Cytometry. The HUVECs were collected and washed three times with cold PBS. They were then incubated and stained with an FITC-Annexin V Apoptosis Detection kit at room temperature for 15 min in the dark. Subsequently, the cells were analyzed by using flow cytometry.

5.8. Statistical Analysis. Statistical analysis was conducted using GraphPad Prism 9, and data were presented as the mean ± SD. One-way ANOVA followed by Tukey multiple comparison tests was used to establish statistical significance. $P < 0.05$ was considered statistically significant.

■ ASSOCIATED CONTENT

Data Availability Statement

All data generated during this study are included in this published article and its supplementary file.

Supporting Information

The Supporting Information is available free of charge at https://pubs.acs.org/doi/10.1021/acsomega.4c10868.

Additional experimental details, including photographs of the results and the raw data, are provided (PDF)

■ AUTHOR INFORMATION

Corresponding Author

Bo Jin − *School of Life Science, Zhejiang Chinese Medical University, Hangzhou 310053, China;* orcid.org/0000-0002-7701-6102; Email: jinbo@zcmu.edu.cn

Authors

Shennan Shi − *School of Life Science, Zhejiang Chinese Medical University, Hangzhou 310053, China*

Yalan Lu − *School of Life Science, Zhejiang Chinese Medical University, Hangzhou 310053, China*

Qiwen Long − *School of Life Science, Zhejiang Chinese Medical University, Hangzhou 310053, China*

Yanqing Wu − *School of Life Science, Zhejiang Chinese Medical University, Hangzhou 310053, China*

Yan Guo − *Hangzhou TCM Hospital Affiliated to Zhejiang Chinese Medical University, Hangzhou 310007, China*

Nipi Chen − *School of Life Science, Zhejiang Chinese Medical University, Hangzhou 310053, China*

Haitong Wan − *School of Basic Medical Sciences, Zhejiang Chinese Medical University, Hangzhou 310053, China;* orcid.org/0009-0005-0776-0269

Complete contact information is available at: https://pubs.acs.org/10.1021/acsomega.4c10868

Author Contributions

S.S.: data curation, formal analysis, investigation, methodology, visualization, writing-original draft. Y.L.: data curation, formal analysis, investigation, methodology, writing-original draft. Q.L.: investigation, methodology, visualization, writing-original draft. Y.W.: data curation, methodology, writing-original draft. Y.G.: visualization, funding acquisition, writing-original draft. N.C.: conceptualization, methodology, writing-original draft. H.W.: project administration, writing-original draft. B.J.: conceptualization, funding acquisition, project administration, resources, supervision, writing-review and editing. S.S. and Y.L. contributed equally to this work.

Notes

The authors declare no competing financial interest.

https://doi.org/10.1021/acsomega.4c10868
ACS Omega 2025, 10, 9604−9612

This study was approved by the Animal Care and Use Committee of Zhejiang Chinese Medical University with ethics approval reference No.20210412.

■ ACKNOWLEDGMENTS

We thank the following for their enthusiastic support in the conduct of the study: the National Natural Science Foundation of China (No. 82374071, No. 82304763); the Natural Science Foundation of Zhejiang Province, China (No.LY23H280006); and the Traditional Chinese Medicine Science and Technology Project of Zhejiang Province of China (No.2024ZR139).

■ REFERENCES

(1) Bi, C.; Li, P. L.; Liao, Y.; Rao, H.-Y.; Li, P.-B.; Yi, J.; Wang, W.-Y.; Su, W.-W. Pharmacodynamic effects of Dan-hong injection in rats with blood stasis syndrome. *Biomed. Pharmacother.* **2019**, *118*, No. 109187.

(2) Chen, J.-R.; Cao, W.-J.; Asare, P.-F.; Lv, M.; Zhu, Y.; Li, L.; Wei, J.; Gao, H.; Zhang, H.; Mao, H.-P.; Gao, X.-M.; Fan, G.-W. Amelioration of cardiac dysfunction and ventricular remodeling after myocardial infarction by danhong injection are critically contributed by anti-TGF-β-mediated fibrosis and angiogenesis mechanisms. *J. Ethnopharmacol.* **2016**, *194*, 559−570.

(3) Chen, J.; Deng, J.; Zhang, Y.-Y.; Yang, J.-H.; He, Y.; Fu, W.; Xing, P.-K.; Wan, H.-T. Lipid-lowering effects of Danhong injection on hyperlipidemia rats. *J. Ethnopharmacol.* **2014**, *154* (2), 437−442.

(4) Duan, Z.-Z.; Li, Y.-H.; Li, Y.-Y.; Fan, G.-W.; Chang, Y.-X.; Yu, B.; Gao, X.-M. Danhong injection protects cardiomyocytes against hypoxia/reoxygenation- and H_2O_2-induced injury by inhibiting mitochondrial permeability transition pore opening. *J. Ethnopharmacol.* **2015**, *175*, 617−625.

(5) Feng, X.-J.; Li, Y.; Wang, Y.-N.; Li, L.-L.; Little, P.-J.; Xu, S.-W.; Liu, S. Danhong injection in cardiovascular and cerebrovascular diseases: Pharmacological actions, molecular mechanisms, and therapeutic potential. *Pharmacol. Res.* **2019**, *139*, 62−75.

(6) Wang, K.-H.; Zhang, D.; Wu, J.-R.; Liu, S.; Zhang, X.-M.; Zhang, B. A comparative study of Danhong injection and Salvia miltiorrhiza injection in the treatment of cerebral infarction: A systematic review and meta-analysis. *Medicine.* **2017**, *96* (22), No. e7079.

(7) Lyu, M.; Yan, C. L.; Liu, H.-X.; Wang, T.-Y.; Shi, X.-H.; Liu, J.-P.; Orgah, J.; Fan, G.-W.; Han, J.-H.; Wang, X.-Y.; Zhu, Y. Network pharmacology exploration reveals endothelial inflammation as a common mechanism for stroke and coronary artery disease treatment of Danhong injection. *Sci. Rep.* **2017**, *7* (1), 15427.

(8) Khan, H.; Kaur Grewal, A.; Gurjeet Singh, T. Mitochondrial dynamics related neurovascular approaches in cerebral ischemic injury. *Mitochondrion.* **2022**, *66*, 54−66.

(9) Plotegher, N.; Filadi, R.; Pizzo, P.; Duchen, M.-R. Excitotoxicity Revisited: Mitochondria on the Verge of a Nervous Breakdown. *Trends Neurosci.* **2021**, *44* (5), 342−351.

(10) Shi, Y.-Y.; Han, L.-J.; Zhang, X.-X.; Xie, L.-L.; Pan, P.-L.; Chen, F. Selenium Alleviates Cerebral Ischemia/Reperfusion Injury by Regulating Oxidative Stress, Mitochondrial Fusion and Ferroptosis. *Neurochem. Res.* **2022**, *47* (10), 2992−3002.

(11) Bresgen, N.; Karlhuber, G.; Krizbai, I.; Bauer, H.; Bauer, H.-C.; Eckl, P.-M. Oxidative stress in cultured cerebral endothelial cells induces chromosomal aberrations, micronuclei, and apoptosis. *J. Neurosci. Res.* **2003**, *72* (3), 327−333.

(12) Qin, W.-W.; Ren, B.; Wang, S.-S.; Liang, S.-J.; He, B.-Q.; Shi, X.-J.; Wang, L.-Y.; Liang, J.-Y.; Wu, F.-H. Apigenin and naringenin ameliorate PKCβII-associated endothelial dysfunction via regulating ROS/caspase-3 and NO pathway in endothelial cells exposed to high glucose. *Vasc. Pharmacol.* **2016**, *85*, 39−49.

(13) Zeisel, S.-H. Antioxidants suppress apoptosis. *J. Nutr.* **2004**, *134* (11), 3179S−3180S.

(14) Zhou, M.-X.; Wei, X.; Li, A.-L.; Wang, A.-M.; Lu, L.-Z.; Yang, Y.; Ren, D.-M.; Wang, X.-N.; Wen, X.-S.; Lou, H.-X.; Shen, T. Screening of traditional Chinese medicines with therapeutic potential on chronic obstructive pulmonary disease through inhibiting oxidative stress and inflammatory response. *BMC Complementary Altern. Med.* **2016**, *16* (1), 360.

(15) Guo, Y.; Yang, J.-H.; Cao, S. D.; Gao, C. X.; He, Y.; Wang, Y.; Wan, H.-T.; Jin, B. Effect of main ingredients of Danhong Injection against oxidative stress induced autophagy injury via miR-19a/SIRT1 pathway in endothelial cells. *Phytomedicine.* **2021**, *83*, No. 153480.

(16) Zhang, L.; Wang, Y.; Li, C.; Shao, C.-Y.; Zhou, H.-F.; Yang, J.-H.; He, Y.; Wan, H.-T. Dan Hong Injection Protects Against Cardiomyocytes Apoptosis by Maintaining Mitochondrial Integrity Through Keap1/Nuclear Factor Erythroid 2-Related Factor 2/JNK Pathway. *Front. Pharmacol.* **2020**, *11*, No. 591197.

(17) Yu, Y.-H.; Kim, G.-W.; Lee, Y.-R.; Park, D.-K.; Song, B.; Kim, D.-S. Effects of Sildenafil on Cognitive Function Recovery and Neuronal Cell Death Protection after Transient Global Cerebral Ischemia in Gerbils. *Biomedicines.* **2024**, *12* (9), 2077.

(18) Chen, S.-M.; Zhang, J.-H.; Li, M.; Zhou, J.; Zhang, Y.-Y. Danhong injection combined with tPA protects the BBB through Notch-VEGF signaling pathway on long-term outcomes of thrombolytic therapy. *Biomed. Pharmacother.* **2022**, *153*, No. 113288.

(19) Liang, L.; Yi, X.-L.; Wang, C.-F.; Su, L.; Wei, G.-J. The Impact of miR-34a on Endothelial Cell Viability and Apoptosis in Ischemic Stroke: Unraveling the MTHFR-Homocysteine Pathway. *Clin. Invest. Med.* **2024**, *47* (3), 27−37.

(20) Tucka, J.; Yu, H.; Gray, K.; Figg, N.; Maguire, J.; Lam, B.; Bennett, M.; Littlewood, T. Akt1 regulates vascular smooth muscle cell apoptosis through FoxO3a and Apaf1 and protects against arterial remodeling and atherosclerosis. *Arterioscler., Thromb., Vasc. Biol.* **2014**, *34* (11), 2421−2428.

(21) You, D.; Xin, J.; Volk, A.; Wei, W.; Schmidt, R.; Scurti, G.; Nand, S.; Breuer, E.-K.; Kuo, P.-C.; Breslin, P.; Kini, A.-R.; Nishimura, M.-I.; Zeleznik-Le, N.-J.; Zhang, J. FAK mediates a compensatory survival signal parallel to PI3K-AKT in PTEN-null T-ALL cells. *Cell Rep.* **2015**, *10* (12), 2055−2068.

(22) Li, Y.-Z.; Yin, H.; Yuan, H.-X.; Wang, E.-H.; Wang, C.-M.; Li, H.-Q.; Geng, X.-D.; Zhang, Y.; Bai, J.-W. IL-10 deficiency aggravates cell senescence and accelerates BLM-induced pulmonary fibrosis in aged mice via PTEN/AKT/ERK pathway. *BMC Pulm. Med.* **2024**, *24* (1), 443.

(23) Zhong, C.-H.; Li, X.-L.; Tao, B.; Peng, L.-L.; Peng, T.-M.; Yang, X.-B.; Xia, X.-G.; Chen, L.-G. LIM and SH3 protein 1 induces glioma growth and invasion through PI3K/AKT signaling and epithelial-mesenchymal transition. *Biomed. Pharmacother.* **2019**, *116*, No. 109013.

(24) Jiang, R.-B.; Guo, Y.; Chen, N.-P.; Gao, C.-X.; Ding, Z.-S.; Jin, B. Total Flavonoids from Carya cathayensis Sarg. Leaves Alleviate H9c2 Cells Hypoxia/Reoxygenation Injury via Effects on miR-21 Expression, PTEN/Akt, and the BCL-2/BAX Pathway. *J. Evidence-Based Complementary Altern. Med.* **2018**, *2018*, 8617314.

(25) Browne, G.; Nesbitt, H.; Ming, L.; Stein, G. S.; Lian, J. B.; McKeown, S. R.; Worthington, J. Bicalutamide-induced hypoxia potentiates RUNX2-mediated BCL-2 expression resulting in apoptosis resistance. *Br. J. Cancer.* **2012**, *107* (10), 1714−1721.

(26) Brunelle, J.-K.; Letai, A. Control of mitochondrial apoptosis by the BCL-2 family. *J. Cell Sci.* **2009**, *122* (Pt 4), 437−441.

(27) Yi, X.-J.; Wang, F.-G.; Feng, Y.; Zhu, J.-F.; Wu, Y.-J. Danhong injection attenuates doxorubicin-induced cardiotoxicity in rats via suppression of apoptosis: network pharmacology analysis and experimental validation. *Front. Pharmacol.* **2022**, *13*, No. 929302.

https://doi.org/10.1021/acsomega.4c10868
ACS Omega 2025, 10, 9604−9612